MERITS OF COMBINATION OF ACTIVE AND PASSIVE MICROWAVE SENSORS FOR DEVELOPING ALGORITHMS OF SST AND SURFACE WIND SPEED

Akira Shibata and Hiroshi Murakami

Japan Aerospace Exploration Agency
Earth Observation Research Center

shibata.akira@jaxa.jp
murakami.hiroshi.eo@jaxa.jp

ABSTRACT ... In developing algorithms to retrieve the sea surface temperature (SST) and sea surface wind speed from the Advanced Microwave Scanning Radiometer (AMSR) aboard the AQUA and the Advanced Earth Observation Satellite-II (ADEOS-II), data from the SeaWinds aboard ADEOS-II were helpful. Since features of the ocean microwave emission (Tb) related with ocean wind are not well understood, in case of using only AMSR data, combination of AMSR and SeaWinds revealed pronounced features about the ocean Tb. Two results from combinations of the two sensors were shown in this paper. One result was obtained at wind speeds over about 6m/s, in which the ocean Tb varies with the air-sea temperature difference, even though the SeaWinds wind speed is fixed at the same values. The ocean Tb increases as the air-sea temperature difference becomes negative, i.e., the boundary condition becomes unstable. This result indicates that the air temperature should be included in AMSR SST algorithm. The second result was obtained from comparison of two wind speeds between AMSR and SeaWinds. There is a small difference of two wind speeds, which might be related with several mechanisms, such as evaporation and plankton.

KEY WORDS: AMSR, SeaWinds, air-sea temperature difference, evaporation, plankton.

1. INTRODUCTION

Passive microwave radiometers observe the microwave emission from the Earth, and active microwave scatterometer measures the returned echo from the Earth. Combination of data from the two sensors has a merit of analyzing physical mechanism of microwave emission and scattering on the Earth, and also of developing algorithms of retrieving the sea surface temperature (SST) and sea surface wind speed. On the Advanced Earth Observing Satellite-II (ADEOS-II), launched by the Japan Aerospace Exploration Agency (JAXA) on Dec. 14, 2002, these passive and active sensors were loaded simultaneously: one is the Advanced Microwave Scanning Radiometer (AMSR), and the other is a NASA scatterometer SeaWinds. The AMSR was made by JAXA (Kawanishi et al., 2003). The SeaWinds was made by NASA (Liu, 2002).

In this paper, we analyze combined data of AMSR and SeaWinds on the ocean surface. To understand mechanisms of the microwave emission and scattering on the ocean surface, we must know an ocean status responding to the ocean wind. The ocean wind varies quickly both spatially and temporally, and it is difficult to observe the ocean wind accurately. Primary purpose of SeaWinds is to measure ocean wind vectors (Liu, 2002). As a result, we can understand the features of ocean microwave emission (Tb) related to the ocean wind, combing the SeaWinds data with the AMSR.

We see two results from combing the AMSR and SeaWinds data. The first is that the ocean Tb varies with the air-sea temperature difference at wind speeds larger than 6m/s. This result indicates that the air temperature should be included in AMSR SST algorithm. The second is obtained from comparison of the AMSR and SeaWinds wind speed. There is a small difference between the two wind speeds, and evaporation and plankton might induce the difference

2. SENSORS AND DATA

AMSR is a forward-looking, conically scanning radiometer positioned at a constant-incidence angle of 55° (Kawanishi et al., 2003). The AMSR frequencies are 6, 10, 18, 23, 36, 50, 52, and 89 GHz. There are two polarizations (v-pol and h-pol) at all frequencies except for 50 and 52 GHz, but only v-pol at 50 and 52 GHz. The diameter of AMSR's main antenna is 2m with a rotation of 40 rpm. The spatial resolution on the Earth's surface at 6 GHz is 40 × 70 km, and 3 × 6 km at 89 GHz.

The SeaWinds emits microwave signals and measures backscattered signals from the Earth's surface. The signal from the ocean surface is related to capillary waves or short gravity waves with a wavelength of several centimeters on the ocean surface. The ocean wind vector (speed and direction) can be retrieved by the scatterometer model function relating the signal with buoy wind data (Liu, 2002; Ebuchi, 2006). We used the Level 2B geophysical data of SeaWinds with a spatial resolution of 25km. ADEOS-II data were available for seven months from April to October 2003.

In this study, air temperature on the ocean surface is necessary, but it is one of most difficult parameters observable from satellite sensors. So, air temperature was

adopted from the weather-forecast model of the Japan Meteorological Agency (JMA), known as the Global Analysis (GANAL). The spatial resolution of the GANAL is 1.25° in both longitude and latitude directions. SST data were adopted from the Reynolds SST of weekly analysis (Reynolds and Smith, 1994). The spatial resolution of the Reynolds SST is 2°.

3. EFFECT OF AIR-SEA TEMPERATURE DIFFERENCE ON THE OCEAN TB

The ocean Tb may be affected by the air-sea temperature difference, and the present section aims to retrieve a relation between the ocean Tb and air-sea temperature difference, using the AMSR and SeaWinds data. To do this, we remove two main effects from the AMSR Tbs: the atmospheric effect, and the SST effect. Equation (1) defines 6V(H)* at 6 GHz, which are free from these two effects.

$$6V(H)^* = AMSR\_6V(H) - atmos\_effect\_6V(H) - calm\_ocean\_6V(H), \quad (1)$$

where AMSR6V(H) is the AMSR Tb at 6 GHz, atmos_effect_6V(H) is the atmospheric correction at 6 GHz, and calm_ocean_6V(H) is the ocean Tb at 6GHz under calm conditions. The parameter, atmos_effect_6V(H), is given by specifying AMSR 23V, AMSR 36V, and SST, and it removes the effects by the water vapor, oxygen, and cloud liquid water in the atmosphere. It also excludes rainy areas by setting the upper limit of atmos_effect_6V(H). The parameter, calm_ocean_6V(H), is defined as SST×(1-r), where r is the Fresnel reflection coefficient with v-pol and h-pol. A detailed explanation of these two parameters was presented in the paper (Shibata, 2006). Units of 6V(H)* are Kelvin. 6V(H)* represent the ocean Tb change from the calm condition, induced by the ocean surface wind, or possibly by the air-sea temperature difference.

To analyze 6V(H)*, we took monthly averages of 6V(H)*, for a purpose of understanding global behaviors of Tbs. In taking the monthly averages, we divided global data according to five categories. The first one is SST, and we divided data into three SST: 5°C (2.5 to 7.5°C), 15°C (12.5 to 17.5°C), and 25°C (22.5 to 27.5°C). The second one is the satellite orbit, and we divided data into the ascending and descending orbits. On the ascending orbits, the AMSR viewed northward. Among the AMSR viewing angles, data at azimuth angles between –20° (or 340°) and 20° were used, in which 0° corresponds to north. On the descending orbits, the AMSR viewed southward. Data at azimuth angles between 160° and 200° were used, in which 180° corresponds to south. The third one is the relative wind direction, which is defined as a relative angle between the AMSR viewing direction and SeaWinds wind direction. The up-wind direction is defined by angles between –20° and 20°, in which 0° corresponds to an opposite direction. The cross-wind direction is defined between 70° and 110° (also 250° and 290°), and the downwind one is between 160° and 200°. The fourth one is the hemisphere, and we divided data into the northern and southern hemispheres. The fifth one is the SeaWinds wind speed, and we divided data to eleven wind speeds from 6m/s to 16 m/s with 1m/s interval. Finally, we took monthly averages for seven months from April to October 2003, according to five categories described above:

We also averaged the air-sea temperature difference monthly for seven months using the GANAL air temperature and Reynolds SST. The averaging was made according to two categories: SST and hemisphere. In addition, it was averaged according to three wind directions (northerly, southerly, and easterly/westerly winds), using the GANAL wind direction. The northerly wind direction implies the azimuth angles between –30° (or 330°) and 30° in which 0° corresponds to north; the southerly between 150° and 210° in which 180° corresponds to south; the easterly between 60 and 120 degrees; and the westerly between 240° and 300°.

Figure 1 compares monthly averaged 6H* and the air-sea temperature difference, in three relative wind directions and at three SST, which are all at the SeaWinds wind speed of 14m/s. In Fig. 1, we find a negative correlation between 6H* and air-sea temperature difference, i.e., 6H* decreases as the air-sea temperature increases. We also find a similar relation between 6V* and air-sea temperature difference.

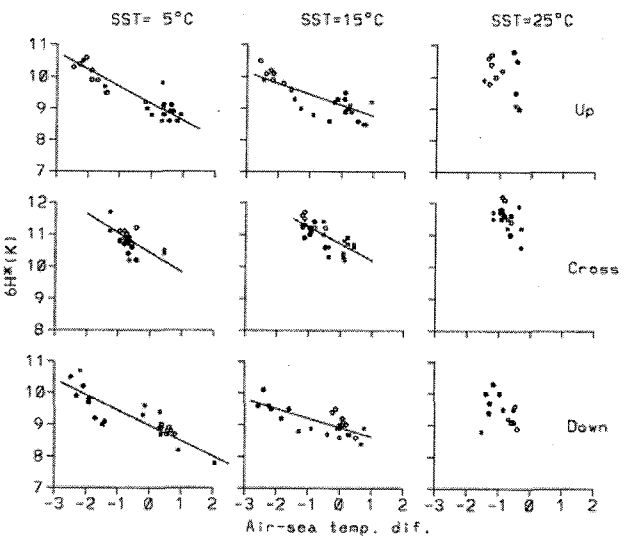

Fig. 1 Relation between 6H* and air-sea temperature difference

. From Fig. 1, we assume that 6V(H)* is linearly related to the air-sea temperature, as defined by Eq. (2).

$$6V(H)^* = a - b \times \Delta T \quad (2)$$

Here, ΔT is the air-sea temperature difference. Coefficients a and b in Eq. (2) were listed in Table 1. Coefficients were determined independently at 5° and 15°C SST, also in three relative wind directions. Regression lines at 25°C SST were not obtained since the air-sea temperature ranges narrowly at 25°C SST.

		up	cross	down
6V*	5°C	3.44 0.38	2.97 0.51	2.15 0.45
	15°C	3.45 0.24	3.19 0.44	2.29 0.28

		up	cross	down
6H*	5°C	9.15 0.54	10.42 0.61	8.98 0.48
	15°C	9.10 0.34	10.71 0.53	8.82 0.30

Table 1 a and b for 6V(H)* (upper; a, lower; b)

We apply our results to a wind effect correction used in the AMSR SST algorithm. Figure 2 shows a thematic technique of the wind correction, in which the 6V*-6H* relation is depicted. A thin line indicates its relation determined in the global ocean in the down-wind direction The AMSR SST is retrieved from 6V*, since the sensitivity of 6V* to SST is greater as twice than the one of 6H*. 6H* is used to remove the wind effect on 6V*.

The 6V*-6H* relation in Fig. 2 indicates that 6V* remains 0K until 6H* reaches at z0, and it increases with the slope of sp above z0. Therefore, a wind correction on 6V*, inc_6V, is given by Eq. (3), using 6H*.

$$\begin{aligned} \text{inc\_6V} &= 0 \qquad \text{for 6H* less than z0,} \\ &= (\text{6H*} - \text{z0}) \times \text{sp} \quad \text{for 6H* greater than z0} \end{aligned} \tag{3}$$

where sp is a slope of 6V* to 6H*, and given by Eq. (4).

$$\text{sp} = \text{6V*}/(\text{6H*}-\text{z0}) \tag{4}$$

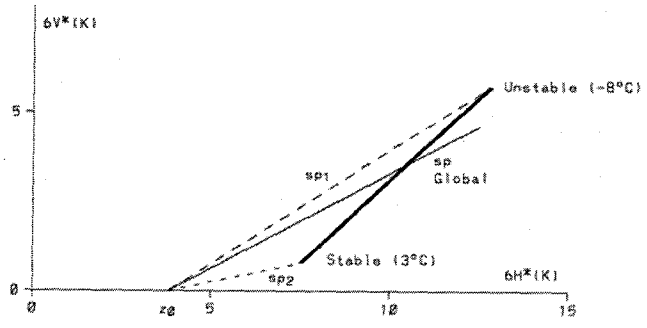

Fig. 2 Thematic figure for the wind correction

In Fig. 2, additional slopes in two cases of negative and positive air-sea temperature difference are shown. The slope of sp_1 represents the negative (unstable) air-sea temperature difference, and its slope is calculated using Eqs. (2) and (4) with ΔT of -8°C. The one of sp_2 represents the positive (stable) one, and it is calculated with ΔT of 3°C. A solid bold line represents positions of 6V* and 6H* with varying ΔT from -8°C to 3°C. Fig. 2 implies that sp should be varied with the air-sea temperature difference ΔT.

4. DIFFERENCE OF WIND SPEEDS BETWEEN AMSR AND SEAWINDS

AMSR 6H* defined by Eq. (1) is closely related with the ocean wind, and also with the SeaWinds wind. We correlate 6H* and SeaWinds wind speed, and show results in Figure 3. A bold line represents the cross-wind direction. Two thin lines represent the down- and up-wind direction, though they are overlapped closely. From Fig. 3, we can convert 6H* to the SeaWinds wind speed, using the SeaWinds wind direction. We call a converting function as f(6H).

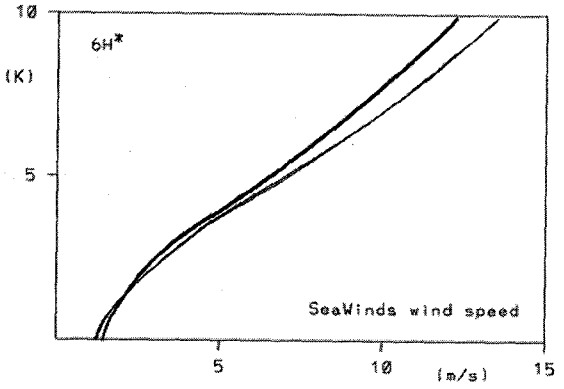

Figure 3 Relation between 6H* and SeaWinds wind speed

Figure 4 shows a difference between the SeaWinds and AMSR wind speeds. The AMSR wind speed is calculated by f(6H*) using the SeaWinds wind direction. The differences shown in Fig. 4 are averaged values during seven months from April to October 2003, and unit is m/s. We can see several features related with some ocean phenomena, such as an evaporation and plankton. We would like to check their relations in the Indian Ocean, where the concentration of the plankton is relatively low.

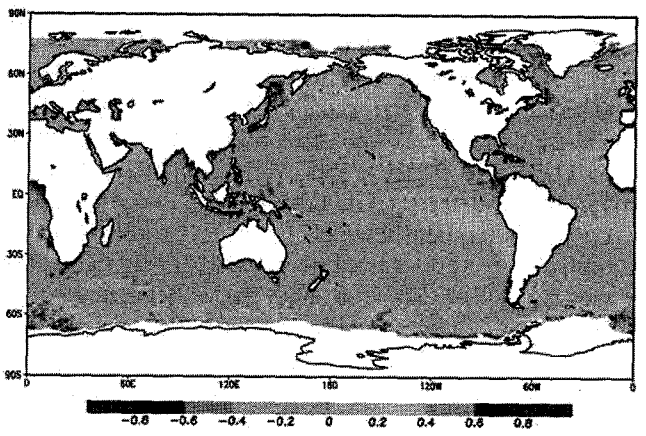

Fig. 4 Difference of SeaWinds and AMSR wind speeds

The evaporation, Ep, is defined by Eq. (5).

$$\text{Ep} = C_D \times (\text{Vs} - \text{Va}) \times \text{Ws}, \tag{5}$$

where C_D is a drag coefficient, Vs saturated humidity corresponding to the SST, Va humidity in the atmosphere above the ocean surface, and Ws wind speed. Unit of evaporation is mm/hour.

Figure 5 compares the wind speed difference and evaporation in the Indian Ocean in April 2003. Two patterns resemble with each other, in particular, in the Arabian Sea, Red Sea. Furthermore, a band crossing along the latitude of 25S is found in both figures. Fig. 6 compares the two in August 2003. Patterns in the Mediterranean Sea resemble with each other. Those in the northern-western ocean off the Australia also do. But, a strong positive difference is found in the Arabian Sea and along the African coast. The plankton may induce this pattern. Figure 7 depicts the chlorophyll-a concentration (unit; mg/m^3) in August 2003, which was retrieved from the Global Imager (GLI) aboard the ADEOS-II. The effect of the plankton is also found in the Okhotsk Sea in Fig. 4.

Mechanisms inducing the difference of the two winds may be different between the evaporation and plankton, and will be discussed elsewhere.

5. CONCLUSION

Combination of the AMSR and SeaWinds data gives a valuable result in analysing the ocean Tb of the AMSR. The ocean Tb varies quickly by the ocean wind, and the simultaneous SeaWinds observations of the wind speed and direction are useful. Though the ADEOS-II data were available for seven months, they would be valued in future.

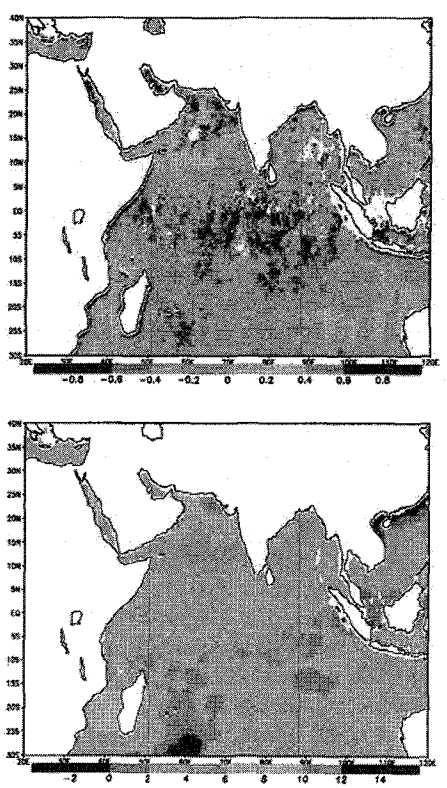

Fig. 5 Comparison of wind difference (upper) and evaporation (lower) in the Indian Ocean in April 2003

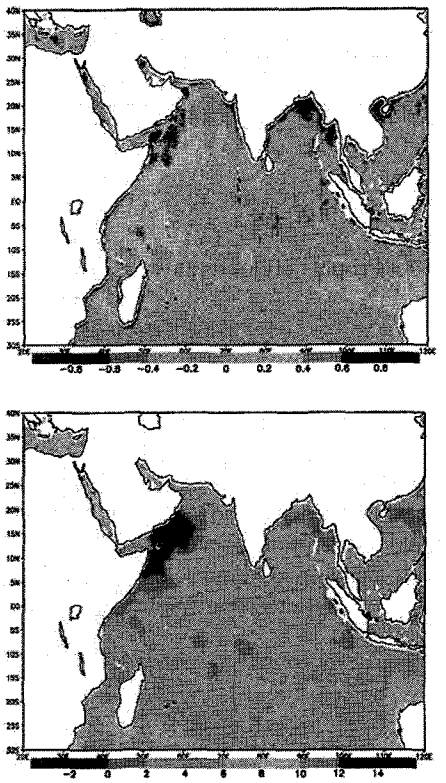

Fig. 6 Same as Fig. 5, but in August 2003

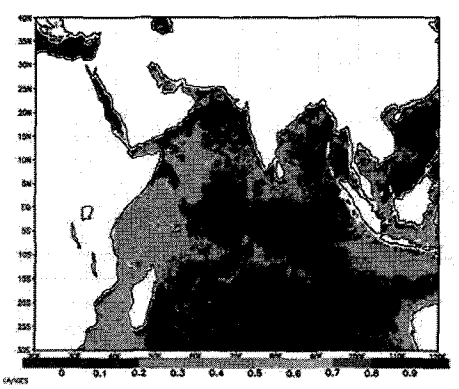

Fig. 7 Chlorophyll-a concentration in August 2003

Acknowledgements

This work was supported by the ADEOS-II project with JAXA EORC.

References

Ebuchi, N., 2006, Evaluation of marine surface winds observed by SeaWinds and AMSR on ADEOS-II, *J. Oceanogr.*, **62**, 293-302.

Kawanishi, T., et al., 2003, The Advanced Microwave Scanning Radiometer for the Earth Observing System (AMSR-E), NASDA's contribution to the EOS for global energy and water cycle studies, *IEEE Trans Geosci. Remote Sensing*, **41**, 184-194.

Liu W. T., 200, Progress in scatterometer application, *J. Oceanograp.*, **58**, 121-136.

Reynolds R. W. and T. M. Smith (1994): Improved global sea surface temperature analyses, *J. Climate*, **7**, 929-948.

Shibata, A., 2006, Features of ocean microwave emission changed by wind at 6GHz, *J. Oceanogr.*, **52**(3), 321-330.